JOURNAL OF MATERIALS SCIENCE 16 (1981) 211–220

Some electrical characteristics of lithium and yttrium sialons

R. I. SHARIF*, J. S. THORP, S. A. KAVANAGH
Department of Applied Physics and Electronics, University of Durham, Durham, UK

Some electrical properties of hot-pressed lithium sialons, $Li_{x/8}Si_{6-3x/4}Al_{5x/8}O_xN_{8-x}$ having $x < 5$ and an yttrium sialon were measured between 291 and 775 K; the former consisted essentially of a single crystalline phase whereas the latter contained 98% glassy phase. For lithium sialons, the charging and discharging current followed a $I(t) \propto t^{-n}$ law with $n = 0.8$ at room temperature. The d.c. conductivities were about 10^{-13} ohm^{-1} cm^{-1} at 291 K and rose to 5×10^{-7} ohm^{-1} cm^{-1} at 775 K. At high temperatures electrode polarization effects were observed in d.c. measurements. The variation of the conductivity over the frequency range 200 Hz to 9.3 GHz followed the $\sigma'(\omega) \propto \omega^n$ law. The data also fitted the "Universal dielectric law", $\epsilon''(\omega) \propto \omega^{n-1}$ well, and approximately fitted the Kramers–Kronig relation $\epsilon''(\omega)/\epsilon'(\omega) - \epsilon_\infty = \cot(n\pi/2)$ with n decreasing from 0.95 at 291 K to 0.4 at 775 K. The temperature variations of conductivities did not fit linearly in Arrhenius plots. Very similar behaviour was observed for yttrium sialon except that no electrode polarization was observed. The results have been compared with those obtained previously for pure sialon; the most striking feature revealed being that $\sigma_{d.c.}$ for lithium sialon can be at least 10^3 times higher than that of pure sialon. Interpretation of the data in terms of hopping conduction suggests that very similar processes are involved in all three classes of sialon.

1. Introduction

Sialon ceramics, made by hot-pressing α-Si_3N_4 and α-Al_2O_3 have been established as materials with many potential high temperature engineering applications. Some of their electrical properties have been reported recently by Thorp and Sharif [1–4]. The preparative techniques have been further extended by Jack [5] to make lithium sialons and yttrium sialon, some of whose chemical and physical properties have been reported by Jama [6].

One of the interests in lithium sialon is that it might be suitable as a solid electrolyte for high voltage cells if compositions could be made which exhibit electrical conductivity values, at room temperature, comparable with silver or sodium-substituted beta-alumina. The interest in yttrium sialon arose out of a general difficulty encountered in preparing ceramics by hot-pressing. If yttria, Y_2O_3, is used as the additive in place of magnesia, a more refractory grain boundary phase is achieved. Yttrium sialon is noteworthy in that it is made of almost entirely glassy phase material, i.e. about 98% glassy phase, the remainder being a crystalline β'-sialon phase. This feature distinguishes it from pure sialons and lithium sialons all of which are predominantly crystalline. In this paper the d.c. field, temperature and frequency dependence of electrical properties for 30 mol% lithium sialon and 14.3 mol% yttrium sialon glass are described. A comparison of the results of pure and doped sialons was made in an attempt to relate the compositions and electrical properties.

2. Experimental procedure

2.1. Preparation and analysis

The original approach towards making lithium sialons was to use a "pure sialon" mix and hot-

* Present address: Department of Applied Physics and Electronics, University of Dacca, Bangladesh.

0022–2461/81/010211–10$03.00/0

press it with lithia, Li_2O. This proved undesirable since Li_2O volatilizes readily causing large weight losses and hence the exact composition of the product was not easily predictable. However, various lithium aluminates (which do not volatilize so readily) can be used instead of lithia. The lithium sialons used here were produced by reacting silicon nitride and lithium aluminospinel ($LiAl_5O_8$). They are isostructural with β-Si_3N_4 and similar to the β-phase produced in the Si–Al–O–N system. Their compositions have been represented by

$$Li_{x/8}Si_{6-3x/4}Al_{5x/8}O_xN_{8-x} \qquad (1)$$

where x and $(8-x)$ are respectively the numbers of oxygen and nitrogen atoms in the unit cell, in which x has a limiting value of about 5. The structures, compositions and phases of lithium sialons have been discussed by Jack [5]. For the present work a range of sialons of different nominal lithium content was prepared and analyses for lithium were undertaken using atomic absorption spectroscopy. The majority of the analyses were made in collaboration with the Department of Chemistry, University of Durham.

In outline the method of analysis adopted was as follows. Samples were first crushed and sieved to provide 53 micron powder. It was then necessary to produce a clear solution from the powder; this proved to be extremely difficult. The most satisfactory method of dissolving the powdered sample was to fuse it with Na_2Co_3 and then acidify the melt with HCl. This gave a clear solution. The solution was then analysed using conventional atomic absorption spectroscopy for lithium, silicon and aluminium. The errors associated with these analyses occurred when trying to obtain solutions of the powders and the overall accuracy of the chemical analysis was estimated as $\pm 0.1\%$ of the weight of element found. For comparison purposes one specimen was also analysed by the Analytical Services Laboratory, Imperial College of Science and Technology, whose results were in excellent agreement with those found here. The nominal compositions of the lithium sialons, together with the analytical data are given in Table I. There appeared to be a considerable discrepancy between the nominal and actual lithium contents and this precluded the systematic study of the effects of increasing the lithium content. Because of the scarcity of material no attempt was made to analyse the yttrium sialon specimen whose nominal composition was 14.3 mol% Y_2O_3, 28.6 mol% AlN, 57.1 mol% SiO_2.

2.2. Measurement techniques

In the present work, measurements have been made of the effects on electrical conductivity of field, temperature and frequency using the methods developed for the previous studies on sialon ceramics [1–4]. The behaviour of decaying and discharging currents, and of the dielectric constants and losses have also been examined. Some of the preliminary measurements in the higher temperature range (600 to 1300 K) were made using platinum/platinum-paste electrodes but the majority of the data was obtained using thin plate specimens with evaporated gold electrodes.

3. Results

3.1. Polarization effects

Polarization effects were observed only in the lithium sialons, all of which exhibited very similar electrical properties.

In Fig. 1 the temperature variation of d.c. conductivity for 30 mol% lithium sialon, measured under a low applied field, between 537 and 1273 K is shown as a log σ against T^{-1} plot. Readings were taken stepwise both during heating and cooling allowing adequate time at each temperature for the specimen to attain a steady condition. The arrows indicating the mode (heating or

TABLE I Chemical analysis data for lithium sialons, (weight percentages).

Specimen number	Lithium		Aluminium		Silicon	
	Starting composition	Final product	Starting composition	Final product	Starting composition	Final product
1	0.43	0.28	11.15	10.57	47.02	41.86
2	0.46	0.33	8.82	7.6	49.41	43.99
3	1.17	0.99	24.02	22.56	31.59	27.68
4	1.40	0.97	27.89	26.32	16.84	15.84
5	1.46	0.72	28.13	18.57	26.25	33.24
6	1.62	0.79	31.44	20.74	22.39	28.27

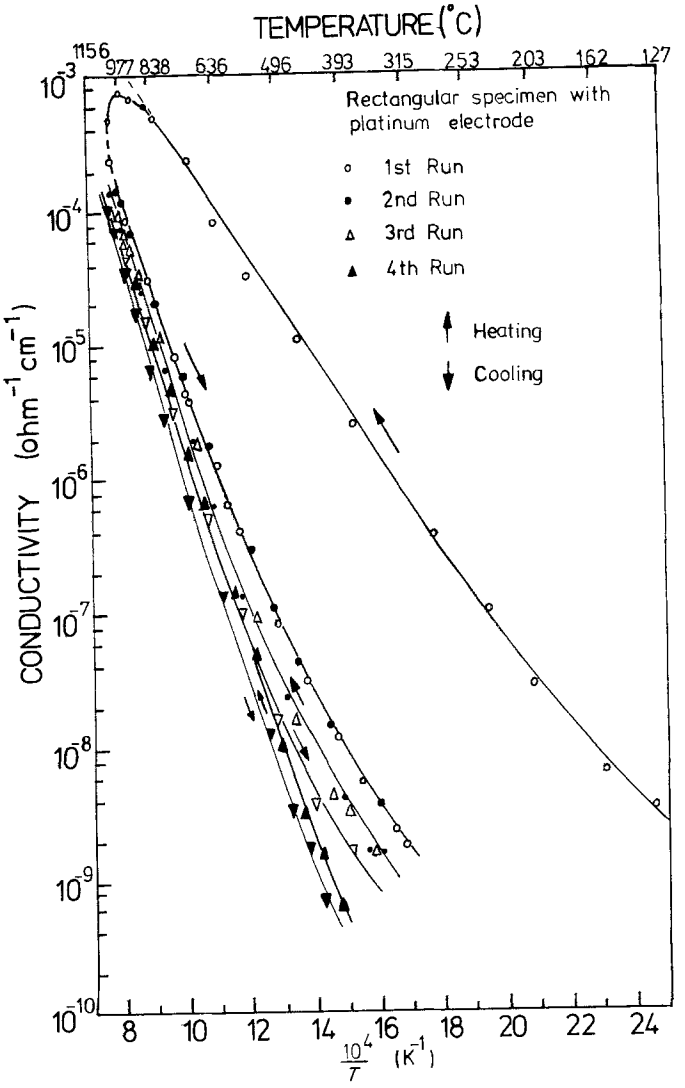

Figure 1 Degradation of d.c. conductivity from the initial steady value for 30 mol% lithium sialon at high temperature.

cooling) in which the data were taken. After the initial run the specimen was left at room temperature (with no field applied) and three further runs were taken after an interval of 24 h. The values of conductivity decreased progressively between successive runs and the results were entirely irreversible. In each run the relationship between log σ and $1/T$ is linear between 700 and 1273 K. The activation energies obtained from the initial and final runs were 0.79 and 1.86 eV respectively. After this series of measurements a colour change in the specimen was observed; the anode became black and the cathode became brown. Electrode polarization effects were observed at high temperatures (but not at low temperatures) and for this reason true values of high temperature conductivity could not be defined.

3.2. Step-function response

The nature of the electrical properties was very similar in lithium and yttrium specimens.

The decay of the total charging currents ($I_C + I_S$), (the charging currents after subtraction of the steady current I and the discharging currents I_D (reverse polarity of I_C) of 30 mol% lithium sialon in step function response under different applied fields at room temperature) are shown in Fig. 2 in which log I is plotted against log t. The initial charging current I_C and discharging current I_D each follows a $I(t) \propto t^{-n}$ law with $n = 0.8$. The time for the current to decay to a steady value (I_S) was 3 h and became shorter with increasing applied field. A slight fluctuation in the decay of charging current is observed around, 10^2 sec. The time of occurrence of the fluctuation region

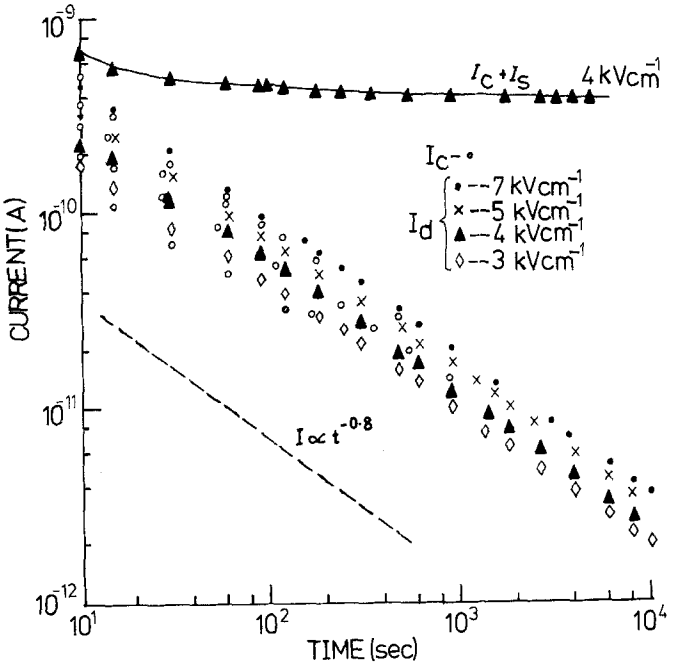

Figure 2 Typical charging currents ($I_C + I_S$), charging currents, I_C (after I_S subtracted) and discharge currents, I_D for 30 mol% lithium sialon under different applied fields at room temperature.

decreases with increasing applied field. The discharging current-densities for different applied fields at $t = 120$ sec are plotted in Fig. 3a which shows that the log J_D against log E^{-k} plot is linear and the value of exponent $k = 0.8$.

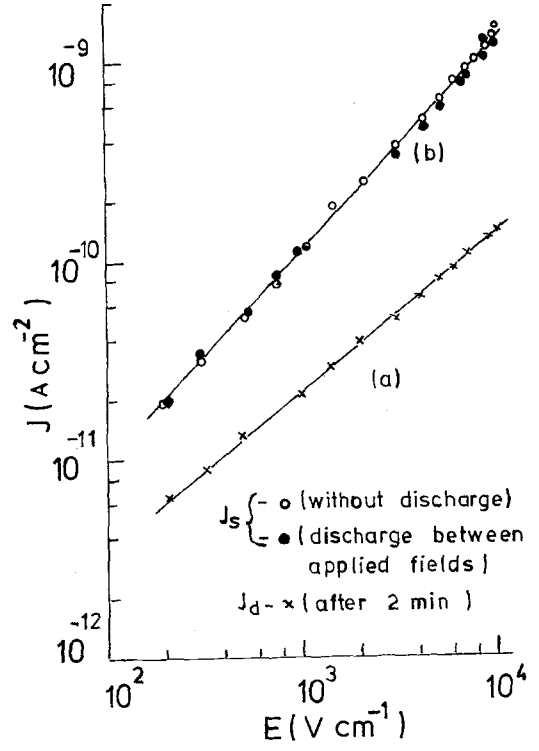

Figure 3 (a) Log J_D against Log E and (b) Log J_S against log E for 30 mol% lithium sialon at room temperature.

The variation of steady current with applied fields at room temperature is shown in Fig. 3. In Fig. 3b the plot of log (J_S) against log E is linear at low electric fields (< 3.8 kV cm^{-1}) and becomes non-linear at moderately high electric fields. The steady currents obtained at different applied fields by the two methods [3, 4] are the same within the limit of experimental error (Fig. 3b); When the same specimen has been used for a very long time no electrode polarization was noticed at room temperature and the results were reproducible.

The temperature variation of conductivity for 30 mol% lithium sialon and 14.3 mol% Y_2O_3 sialon at a low applied field is shown in Fig. 4. The relation between log σ and T^{-1} is linear between 725 and 525 K for the lithium specimen and between 825 and 770 K for the yttrium specimen, it becomes non-linear at lower temperatures. The values of activation energies (E_A) are listed in Table I. The pre-exponential factor was calculated from the linear high temperature region and gives $\sigma_0 \sim 1$ ohm^{-1} cm^{-1}.

No Hall voltage was observed in the lithium sialon specimen between 573 and 1200 K under the conditions described in earlier publications [1, 4]. Thus, the estimated Hall mobility is probably less than 10^{-4} cm^2 V^{-1} sec^{-1}; no measurements were attempted on yttrium sialon.

It is noticed that $\sigma_{d.c.}$ for lithium sialon is less than for yttrium sialon at temperatures below 385 K while the former is much higher above

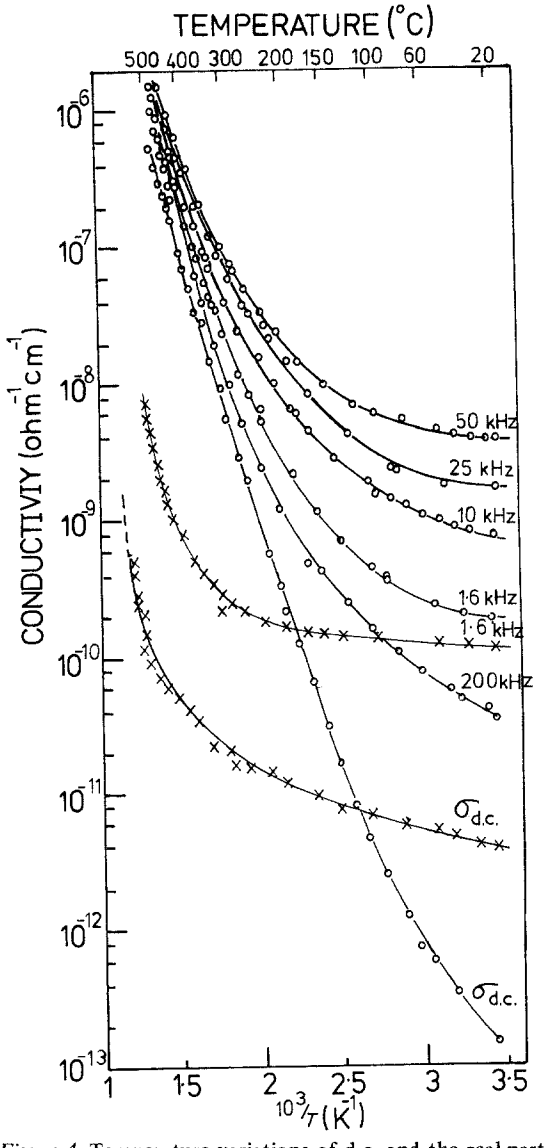

Figure 4 Temperature variations of d.c. and the real part of a.c. conductivities for 30 mol% lithium sialon (○) and 14.3 mol% yttrium oxide sialon glass (×).

that temperature. The conductivities of both materials are at least two to three orders of magnitude higher than that of pure sialon [3, 4] throughout the temperature range. The values of conductivity for the three materials (pure and doped sialons) at 291 and 723 K are listed in Table II for comparison.

3.3. a.c. electrical properties

The frequency variation of the true a.c. conductivity, was deduced from the difference between the experimental data for the real part of conductivity, $\sigma(\omega)$ and the d.c. conductivity $\sigma_{d.c.}$ at room temperature. Over the frequency range 200 Hz to 3 MHz, this fits the relation,

$$\sigma'(\omega) = (\sigma(\omega) - \sigma_{d.c.}) \propto \omega^n \qquad (2)$$

well where n has the values 0.78 for yttrium sialon and 0.9 for lithium sialon; these are also listed in Table II. The apparent ω^2 variation above 5 MHz seems to be spurious and the linear ω^n variation is considered to hold over the whole frequency range from 200 Hz to 9.3 GHz. Similar behaviour was observed previously in pure sialon [2, 4].

The temperature variation of conductivity $\sigma(\omega)$ at different frequencies (up to 50 KHz) is shown in Fig. 4 in which log $\sigma(\omega)$ is plotted against the reciprocal of absolute temperature. The temperature variation of conductivity at different frequencies also fits Equation 2 where the exponent n varies from 0.9 to 0.3, decreasing slowly with increasing temperature. It is significant to note that the temperature variation of conductivity of lithium sialon at different frequencies does not fit in Arrhenius plots linearly and the activation energy must be defined as the gradient of the plots of log σ against T^{-1}. The activation energy decreases with decreasing temperature and increasing frequency. The highest and lowest values of E_A are in the range of 0.88 to 0.02 eV for lithium sialon and 1.1 to 0.016 eV for yttrium sialon. There is a good correlation between the temperature variations of d.c. and a.c. conductivities. At high temperature the values of E_A deduced from a.c. and d.c. measurements are very nearly the same (Table III). The a.c. conductivity data of lithium sialon fitted $\log \sigma(\omega) \propto T$ rather better than $\log \sigma(\omega) \propto T^{-1}$.

In Fig. 5 the observed variation of $\epsilon'(\omega)$ with frequency at room temperature is shown as a log $\epsilon'(\omega)$ against log f plot. The value of $\epsilon'(\omega)$ decreases slightly with frequency up to 6 MHz. Above that frequency, $\epsilon'(\omega)$ increases and this apparent rise is again thought to be spurious because the microwave data fits reasonably on the extrapolation of the low frequency $\epsilon'(\omega)$ variations of both the materials. The values of ϵ' and $\sigma(\omega)$ for yttrium sialon decreased by 20% from initial values during thermal treatments. This behaviour was also observed in high temperature d.c. conductivity. The room temperature value of ϵ' for yttrium sialon at 1.6 KHz was about 16.5 and reduced to 9 after thermal treatment; the value of ϵ' increased to 14 at 725 K. It is noticed that the values of the dielectric parameters of yttrium

TABLE II d.c. electrical parameters for sialons (pure and doped).

Sample	Nominal composition	Conductivity (Ω^{-1} cm^{-1})		Activation energy (eV)		σ_0 (Ω^{-1} cm^{-1}) from high temperature	Room temperature data	
		18° C	450° C	High temperature	Low temperature		Value of n	Drift mobility ($cm^2 V^{-1} sec^{-1}$)
1.	30 mol% lithium sialon	1.3×10^{-13}	3.2×10^{-7}	0.83	0.30	0.5	0.8	2×10^{-7}
2.	14.3 mol% Y_2O_3-sialon	4.4×10^{-12}	1.8×10^{-9}	1.40	0.05	0.26	–	–
References [3, 4]	$z = 3.2$ sialon	1.1×10^{-16}	4.0×10^{-12}	1.45	0.05	0.05	0.7	7.35×10^{-8}

TABLE III Dielectric parameters for sialons (pure and doped).

Temperature (K)	n from $(\epsilon' - \epsilon_\infty)$		n from ϵ''		Measured $(\epsilon''/\epsilon' - \epsilon_\infty)$		Expected value of n $(2/\pi)\cot^{-1}(\epsilon''/\epsilon' - \epsilon_\infty)$	
	Li-sialon	Y-sialon	Li-sialon	Y-sialon	Li-sialon	Y-sialon	Li-sialon	Y-sialon
291	0.96	0.90	0.90	0.78	3.14×10^{-2}	0.224	0.98	0.86
400	0.95	–	0.70	–	0.274	–	0.83	–
500	0.78	–	0.56	–	0.599	–	0.66	–
600	0.65	–	0.44	–	1.20	–	0.44	–
700	0.59	–	0.30	–	2.41	–	0.25	–

sialon at room temperature are higher than those of lithium sialon and they appear to be lowered after thermal treatment (Fig. 5). This lowering is observed only in yttrium sialon but not in the other nitrogen ceramics [1–3]. This effect is significant and will be discussed in Section 4. Even in high temperature dielectric measurements the electrode polarization effect was not observed for lithium sialon and the results could be reproduced.

There is no major difference between the magnitudes of the frequency variation of $\sigma(\omega)$ and $\epsilon'(\omega)$ for lithium, yttrium and pure sialons at room temperature but at high temperature, $\sigma(\omega)$ and $\epsilon'(\omega)$ for pure sialon are at least one to two orders of magnitude lower than that of lithium sialon; the values of the parameters for yttrium sialon are intermediate between them. Some values are listed in Tables III and IV for comparison.

4. Discussion

4.1. Step-function response

The time dependence of the charging current (after substracting I_S) and the discharging current on step-function excitation at different applied fields follow the Universal law of dielectric response [7–10].

$$I(t) \propto t^{-n} \tag{3}$$

with $n < 1$. In the case of lithium sialon the value of n derived from I_C and I_D is 0.8 at room temperature. This behaviour is equivalent to the Universal law of dielectric loss $\epsilon''(\omega) \propto \omega^n$ or $\sigma'(\omega) \propto \omega^n$ [7, 9]. This type of loss is also observed in this material and will be discussed in Section 4.2.

The drift mobility of lithium sialon is about 2×10^{-7} cm^2 V^{-1} sec^{-1}. The drift mobility for pure sialon obtained previously is listed in Table II for comparison.

These very low mobility values (both μ_D and μ_H) suggest that the possible transport mechanism is a hopping process by localized charge carriers e.g. [4].

The low-field steady-current behaviour shows that the log J against log E characteristic is linear

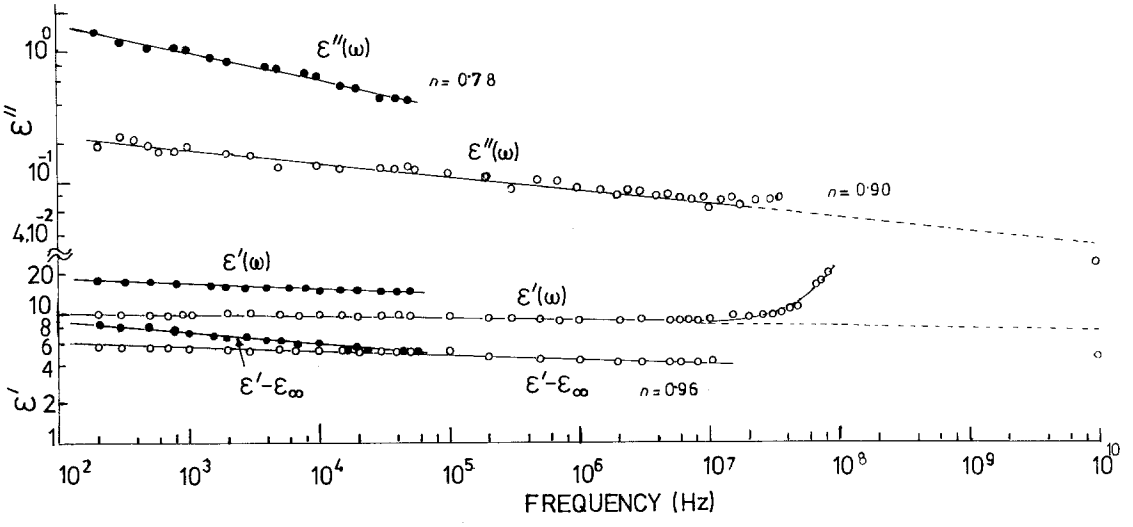

Figure 5 The frequency dependence of dielectric loss $\epsilon''(\omega)$, dielectric constant $\epsilon'(\omega)$ and $(\epsilon' - \epsilon_\infty)$ for 30 mol% lithium sialon (○) and 14.3 mol% yttrium sialon (●) at room temperature.

TABLE IV Dielectric parameters for sialons (pure and undoped)

Sample reference	Dielectric parameters at 1.6 KHz									Microwave at 9.3 GHz (room temperature)	
	$\sigma(\omega)$ ohm^{-1} cm^{-1}		E_A (eV)		$\sigma(\Omega^{-1}$ cm$^{-1})$	tan δ		ϵ'			
	293 K	723 K	High temperature	Low temperature		293 K	723 K	293 K	723 K	tan δ	ϵ'
Li-sialon	1.5×10^{-10}	7×10^{-7}	0.88	0.05	1.16	3×10^{-2}	6.91	9	140	5.22×10^{-3}	4.41
Y-sialon	8×10^{-10}	1.5×10^{-9}	1.03	0.015	0.05	5.2×10^{-2}	2.1×10^{-1}	17; 9	14	2.85×10^{-3}	9.5
References [2, 4] $z = 3.2$ sialon	2×10^{-11}	10^{-9}	1.30	0.05	0.05	2×10^{-3}	9×10^{-3}	8.5	12	4×10^{-2}	5.0

and the magnitude of the slope, (1.03), shows that the Ohm's law is obeyed. At high temperatures, the values of E_A and σ_0 for the two specimens indicate that the conduction is likely to be hopping by carriers excited into the localized states near the edge of the conduction or valence band [12].

At low temperatures, the conductivity of lithium sialon does not fit the relation $T^{-1/4}$ well although it is not linear in the log against T^{-1} plot; moreover, the lowest observed activation energy, $E_A \sim 0.3$ eV does not support this process.

The conductivity degradation of lithium sialon at high temperature could be attributable to some form of solid state electrolysis or diffusion due to Li^+ ions which may be expected to be relatively highly mobile. Electrolysis is likely to be caused by the migration of Li^+ from anode to cathode, which, in the absence of replenishment, depletes the Li^+ ions and leads to decreased conductivity. After electrolysis, when the specimen was disconnected from the circuit, a voltage of the order of 0.2 V was observed, even after 12 days. This standing voltage and the temperature variation of the steady discharge current are strong evidence for electrolysis. The discolourations of the electrodes may be associated with a solid-state electrolytic effect for lithium ions and their corresponding cation vacancies. It may be noted that the crystallographic structures of pure sialon and lithium sialon are very similar and so, if the degradation and colour changes were caused by polarization or densification of the grain boundary glass by thermal treatment or to effects of the electrode materials (gold and platinum), there seems no reason why the effect should only be seen in lithium sialon.

4.2. a.c. behaviour

The frequency dependence of dielectric loss $\epsilon''(\omega)$, calculated from the relation $\epsilon''(\omega) = \sigma'(\omega)/\epsilon_0\omega$ at room temperature, is shown in Fig. 5. Similarly, the temperature variations of $\epsilon''(\omega)$ obtained from the experimental data are shown in Fig. 6. This fits the Universal law of dielectric loss well [7–9]

$$\epsilon''(\omega) \propto \omega^{n-1} \qquad (4)$$

with values of n decreasing from 0.9 at room temperature to 0.35 at 725 K for lithium sialon.

The values of $(\epsilon'(\omega) - \epsilon_\infty)$ for the two specimens, obtained after subtraction of ϵ_∞ at room temperature, is shown in Fig. 5. Similarly, the temperature variations of $(\epsilon'(\omega) - \epsilon_\infty)$ are shown in Fig. 6 as log $(\epsilon'(\omega) - \epsilon_\infty)$ against log f at different temperatures. It is found that these follow [7–9]

$$(\epsilon'(\omega) - \epsilon_\infty) \propto \omega^{n-1} \qquad (5)$$

with values of n decreasing from 0.95 at room temperature to 0.59 at 700 K for lithium sialon. At high temperatures the value of n in the $(\epsilon'(\omega) - \epsilon_\infty)$ variation is higher that the corresponding value in the $(\epsilon''(\omega) \propto \omega^{n-1})$ law. This shows that the ratio of $\epsilon''(\omega)$ to $(\epsilon'(\omega) - \epsilon_\infty)$ is not compatible with the Kramers–Kronig relation [7–9]

$$\epsilon''(\omega)/(\epsilon(\omega) - \epsilon_\infty) = \cot(n\pi/2) \qquad (6)$$

which can apply to either non-Debye dipolar or to hopping charge carriers (ions or electrons) systems. The values of n obtained at different temperatures from the $\epsilon''(\omega)$ and $(\epsilon'(\omega) - \epsilon_\infty)$ variations together with those derived from Equation 6 by substitution of the experimental values of the ratio $\epsilon''(\omega)/(\epsilon'(\omega) - \epsilon_\infty)$ are shown for comparison in Table III. It is also noticed that the value of n in $i \propto t^{-n}$ law is not consistent with the value of n in either $\epsilon''(\omega) \propto \omega^{n-1}$ or $(\epsilon'(\omega) - \epsilon_\infty) \propto \omega^{n-1}$ law at any temperature. This anomalous behaviour does not clearly indicate any particular conduction mechanisms as suggested by Jonscher [7–9].

It is significant that the presence of space change was observed in the samples when the measurements were made at high temperatures and this effect was minimized by giving proper heat treatment [3, 4]. It is therefore, suggested that the space charge effect cannot be ruled out and its presence may prevent the system obeying Equation 6. Alternatively, the d.c. contribution might not have been properly subtracted from ϵ'' and ϵ_∞ from ϵ'.

Evidence for hopping is provided by the fact that no loss peak appears anywhere and the values of n less than 0.5 are seen at high temperatures [7, 13].

Furthermore, the temperature variations of $\sigma(\omega)$ and $\epsilon'(\omega)$ are of the simple Arrhenius type. This feature is characteristic of the hopping conduction [10, 13].

The decrease of conductivities (both d.c. and a.c.) and dielectric constant for yttrium sialon thermal treatment is unlikely to be associated with polarization effects; since no changes of colour or steady discharge current were observed. One possible explanation of this behaviour is that

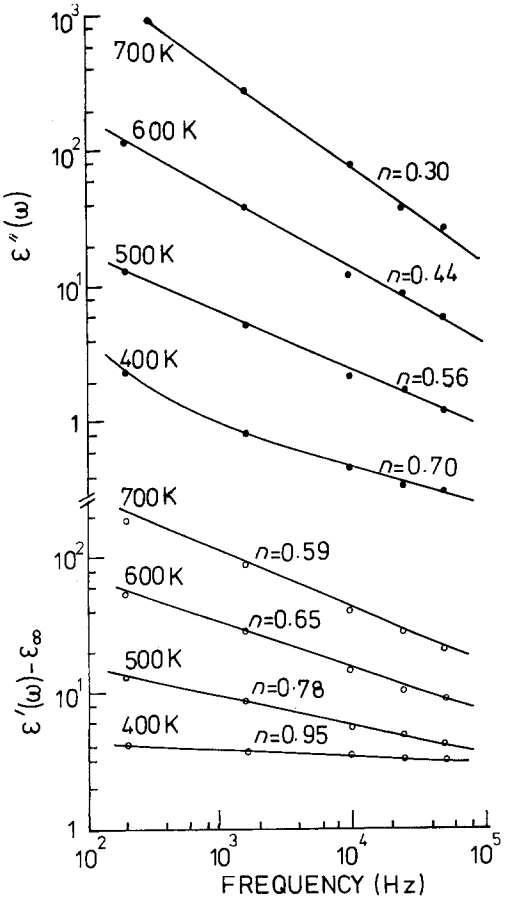

Figure 6 Typical temperature variations of the power law characteristics of (a) $\epsilon''(\omega) \propto \omega^{n-1}$ and (b) $(\epsilon'(\omega) - \epsilon_\infty) \propto \omega^{n-1}$ for lithium sialon.

densification of the glass structure leads to less void space in the glass and so the conductivities and ϵ' are reduced during heating prior to the appearance of the equilibrium crystalline phase. This behaviour has been observed in many glasses and glass ceramics [14].

The conductivities (d.c. and a.c.) and the dielectric constant of the β'-sialon phase are lower than that of lithium sialon and the corresponding values for yttrium sialon glass are intermediate between them; these are listed in Tables II, III and IV. This shows that the chemical composition of the sialon has a marked effect on its conductivity, although the mechanism of conduction is probably very similar in all the materials.

Acknowledgements

We wish to thank the Science Research Council for contract support for this research. We are indebted to Professor K. H. Jack (University of Newcastle-upon-Tyne) and members of this group for supplying specimens and for many helpful discussions. One of us (R.I.S.) also wishes to thank the University of Dacca for the award of a Research Scholarship.

References

1. J. S. THORP and R. I. SHARIF, *J. Mater. Sci.* **11** (1976) 1494.
2. *Idem, ibid.* **12** (1977) 2274.
3. *Idem, ibid.* **13** (1978) 441.
4. R. I. SHARIF, Ph.D. Thesis, University of Durham, 1977.
5. K. H. JACK, *J. Mater. Sci.* **11** (1976) 1135.
6. S. A. B. JAMA, Ph.D. Thesis, University of Newcastle-upon-Tyne, 1975.
7. A. K. JONSCHER, *Phil. Mag. B* **38** (1978) 587.
8. *Idem, Nature* **267** (1977) 673.
9. *Idem, Thin Solid Films* **36** (1976) 1.
10. *Idem* in, "Electrets, Charge storage and Transport in Dielectrics", edited by M. M. Pearlman (Electrochem. Soc. Inc., 1973) p. 269.
11. T. J. LEWIS, "Dielectric Materials, Measurements and Applications" (Institute of Electrical Engineers, London, 1975) p. 261.
12. N. F. MOTT and E. A. DAVIS, "Electronic processes in Non-Crystalline Materials", (Clarendon Press, Oxford, 1971).
13. A. K. JONSCHER and R. M. HILL, *Phys. Thin Films* **8** (1975) 169.
14. D. L. KINSER in "Physics of Electronics Ceramics, Part A", edited by L. L. Hench and D. B. Dove (Marcel Dekker, New York, 1971) p. 523.

Received 13 March and accepted 30 June 1980.